Bull Eng Geol Environ (2015) 74:815–826
DOI 10.1007/s10064-014-0641-5

ORIGINAL PAPER

Assessment of the effect of stress anisotropy on tunnel deformation in the Kaligandaki project in the Nepal Himalaya

Pawan Kumar Shrestha · Krishna Kanta Panthi

Received: 12 April 2014 / Accepted: 16 June 2014 / Published online: 15 July 2014
© Springer-Verlag Berlin Heidelberg 2014

Abstract Most of the analytical approaches that are available for assessing plastic deformation in tunnels that pass through weak, schistose, and foliated rock masses assume an isostatic stress state. However, in situ stresses are seldom isostatic in a tunnel passing through a varying rock overburden. The work reported here analyzed the effect of stress anisotropy on the magnitude of plastic deformation in the Kaligandaki headrace tunnel in the Nepal Himalaya, where extensive deformation monitoring plans were implemented during tunnel excavation. Recorded tunnel deformation, mapped geological information, lab-tested rock mechanical properties, and an approach reported by Hoek and Marinos (Tunn Tunn Int 32(11):45–51, 2000) were used to estimate rock mass parameters. The convergence confinement method (Carranza-Torres and Fairhurst, Tunn Undergr Space Technol 15(2):187–213, 2000) was used to assess the effective support pressure for the known tunnel deformations of 77 tunnel sections assuming an isostatic stress state. Numerical modeling was carried out to assess the effect of stress anisotropy on tunnel deformation. The analysis indicated that CCM overestimates the magnitude of tunnel deformation. This may be explained by the fact that CCM applies for a circular tunnel in the isostatic stress state, which is seldom the case. Actual measured deformations were calibrated using numerical modeling to develop equations that may be used to estimate the plastic deformation of tunnels that are subjected to stress anisotropy. However, it should be emphasized that the proposed equations are based on the data records for a single tunnel, so further validation will be needed using data records of other well-monitored tunnel projects.

Keywords Plastic deformation · Stress anisotropy · Kaligandaki headrace tunnel · Nepal Himalaya

P. K. Shrestha (✉) · K. K. Panthi
Department of Geology and Mineral Resources Engineering, Norwegian University of Science and Technology (NTNU), Sem Sælands Vei 1, 7491 Trondheim, Norway
e-mail: pawan.k.shrestha@ntnu.no

K. K. Panthi
e-mail: krishna.panthi@ntnu.no

Introduction

There are many challenges associated with the construction of tunnels through weak and tectonically deformed rock masses. Stability becomes a concern, particularly when the rock mass is schistose, sheared, folded, and thinly foliated. A tunnel passing through such a plastically deformed rock mass with a high overburden may experience large deformations in the periphery of a tunnel contour. In extreme situations, the tunnel may suffer a partial or full collapse, which may be difficult to handle while tunneling. In order to control excessive deformation and limit tunnel collapses, heavy supports are normally installed in them, and tunnels through rock in the Himalayan region are no exception.

Plastic deformation in the tunnel periphery starts before and immediately after the excavation, and continues even after the rock support has been applied. Since the application of heavy rock support is costly and time-consuming, rock support optimization should be performed in order to limit deformation to an acceptable range. Rock support interaction assessment is normally realized using techniques such as the convergence confinement method (CCM) (Panet 1995, 2001; Carranza-Torres and Fairhurst 2000). The basic assumption of CCM is that the isostatic stress condition holds around a circular tunnel. The

magnitude of the stress is usually given by the vertical gravitational stress (Singh et al. 1992; Goel 1995; Hoek and Marinos 2000). However, isostatic stress equivalent to the magnitude of vertical stress is seldom the case in a tunnel passing through a varying rock overburden (depth). Nonuniformity of in situ stress may lead to a large non-uniform plastic zone around the tunnel. This may eventually result in different degrees of tunnel displacement (closure) around the tunnel contour (Detournay and John 1988; Pan and Chen 1990). Support design that only considers the vertical stress may therefore lead to overestimation.

The work reported in the present paper focused on the assessment of tunnel deformation behavior due to stress anisotropy. The analysis utilized actual measured tunnel deformations, laboratory-tested rock mechanical properties, and mapped geological information for the headrace tunnel of the Kaligandaki A hydroelectric project located in the Nepal Himalaya. Three stages of analysis were performed. Firstly, the rock mass strength was estimated using recorded tunnel deformations, lab-tested rock mechanical properties, and mapped quality records of the rock mass. Secondly, CCM analysis was carried out to evaluate the effective support pressure. Finally, numerical analysis was conducted to assess the impact of stress anisotropy and to check the validity of applying an analytical method (CCM) to a non-circular tunnel subjected to stress anisotropy. Attempts were also made to establish a relationship between tunnel strains, the shear modulus, and the in situ stress state.

Kaligandaki headrace tunnel

The headrace tunnel of the Kaligandaki A hydroelectric project, which is located in the western part of Nepal, is approximately 5,950 m long. The excavated tunnel section is mostly horseshoe (inverted-D) in shape with an excavated diameter of 8.3 m. The tunnel has a cross-sectional area of 58 m^2 excluding a downstream short (360 m) stretch that that has a cross-sectional area of 61.5 m^2.

Geology along the headrace tunnel

The Kaligandaki A project is located in the Lesser Himalayan meta-sedimentary rock formations in close proximity to the Main Central Thrust (MCT) to the north and the Main Boundary Thrust (MBT) to the south. As a result, several local faults such as the Badhighat, Andhikhola, and Kaligandaki faults are close to the project. In fact, a branch of the Andhikhola Fault named the Andhi Fault crosses the headrace tunnel about 700 m from the intake. The headrace tunnel alignment passes mainly through highly schistose and deformed graphitic phyllite and siliceous phyllite (Fig. 1). Generally, the phyllite rock mass along the tunnel is gray to dark gray, moderate to highly weathered, thinly foliated, and fractured. The shear bands of quartz vein are mostly parallel to the foliation planes. The rock mass along the tunnel alignment ranges from extremely poor to fair in quality, with Q values ranging from 0.01 to 3.62 (NEA 2002).

As the project is located in a tectonically active Himalayan region consisting of highly schistose meta-sediments, folding, faulting, and shearing are very common in the rock mass. The orientation and dips of the joint sets are scattered due to folding, meaning that there is no distinct joint system except for the foliation joints (Fig. 2). The orientation of the foliation joints varies greatly along the tunnel alignment, with the general trend being for orientation in the southwest–northeast direction and dipping towards the southwest. Alteration and weathering of the rock mass is considerable and joints are filled with highly sheared clay, quartz, and calcite veins (Panthi 2006; Panthi and Nilsen 2007).

Tunnel excavation and support

The headrace tunnel was excavated from both the upstream and downstream working fronts. 3,150 m of the tunnel were excavated from the upstream working front, whereas the remaining 2,800 m were excavated from downstream. Due to the poor-quality rock mass present, most of the tunnel was excavated using heading and benching. The heading part included an arch and an ~1-m tunnel wall.

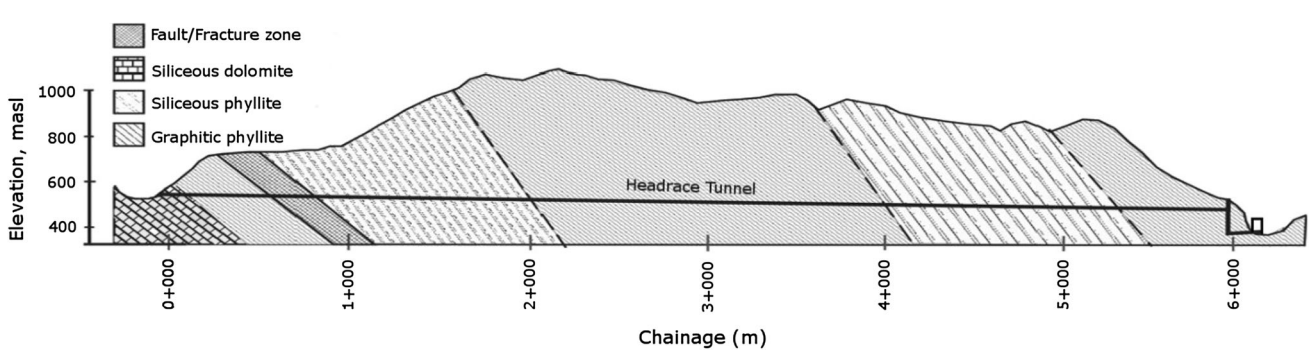

Fig. 1 Geological profile of the Kaligandaki headrace tunnel (Panthi 2006)

Fig. 2 Typical tunnel section showing the schistose and sheared rock mass

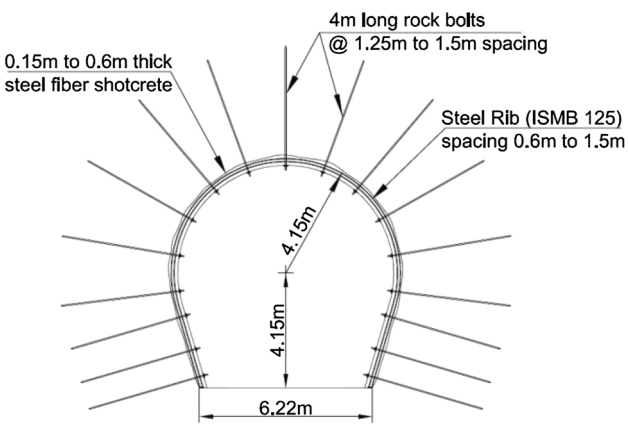

Fig. 3 Typical tunnel section with applied supports

The benching excavation normally had a long lag. However, on some occasions, when the quality of the rock mass improved, heading excavation was stopped until the bench met the tunnel face so that full-face excavation could be performed. The tunnel advance rate varied according to the rock mass conditions and the extent of support applied. When the rock mass was very weak, the advance rate was as low as 0.6 m/day, whereas it went up to 3 m/day when favorable rock mass conditions were present. The overall average tunnel advance rate was slightly above 1 m/day.

Since the rock mass was of poor to extremely poor quality, the tunnel contour deformed to varying extents. The degree of deformation depended upon the magnitude of the in situ stress and the quality of the rock mass. Extensive rock support was applied to avoid complete tunnel collapse. The preliminary rock support that was commonly applied consisted of steel ribs of ISMB125 spaced 0.6–1.5 m apart, steel-fiber-reinforced shotcrete of thickness 0.15–0.6 m, and grouted rock bolts 4 m long and 25 mm in diameter (Fig. 3). Spilling bars 25 mm in diameter were also used in limited stretches of the tunnel when the rock mass was of exceptionally poor quality. After the tunnel had been fully excavated it was supported by a full concrete lining. The headrace tunnel became fully operational by the end of 2001.

Table 1 Summary of in situ stress in the Kaligandaki headrace tunnel

Description	Vertical stress (σ_v) (MPa)	In-plane horizontal stress (σ_{hi}) (MPa)	Out-plane horizontal stress (σ_{ho}) (MPa)	In-plane stress ratio (k)
Minimum	6.20	2.45	3.12	0.22
Average	13.79	3.30	3.96	0.25
Maximum	16.86	3.64	4.30	0.40

In situ stress condition

The instability of a tunnel through a highly schistose rock mass is greatly influenced by the in situ stress magnitudes and their orientations. The higher the magnitude of the stress, the greater the potential for plastic deformation (squeezing) in the periphery of the tunnel. At the Kaligandaki headrace tunnel, the overburden varies from 35 m to as high as 625 m, with an average overburden of 400 m, which is considerable for a tunnel passing through a highly schistose rock mass. The vertical stress caused by the overburden is as high as 17 MPa, with an average value of approximately 14 MPa. Compared to the vertical stress magnitude, horizontal stress magnitudes in the tunnel were found to be rather low. One of the causes of low horizontal stress magnitudes is a low value of Poisson's ratio, which is close to 0.1 according to Panthi (2006). This means that the gravity-led horizontal stress component corresponds to almost one-tenth of the vertical overburden stress. In addition, the horizontal stress magnitudes are greatly influenced by tectonic activity (Panthi 2012).

Rock stress measurements carried out at Kaligandaki (Nepal 1999) showed that the tectonic stress component at this project is approximately 3 MPa. Following Panthi (2012), the general orientation of the direction of tectonic movement in the Central Himalaya is close to north–south. The Kaligandaki project is located in the Central Himalaya and the headrace tunnel has a trend of 144–324°, making an angle of approximately 36° with the direction of tectonic stress. This gives resolved horizontal tectonic stress magnitudes in the tunnel of 1.76 MPa in-plane and 2.4 MPa out-of-plane. Table 1 summarizes the estimated in situ stress magnitudes along the tunnel at places where displacement monitoring was carried out (i.e., between headrace tunnel chainages 739 and 5,200 m). As seen in

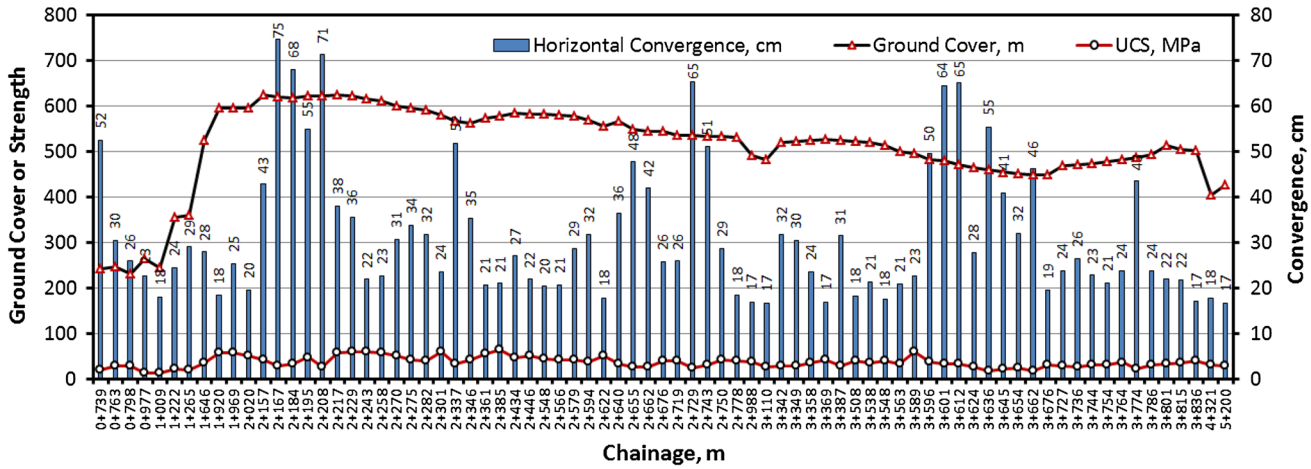

Fig. 4 Tunnel convergence, ground cover, and back-calculated uniaxial compressive strength of the intact rock at various chainages

Table 1, the vertical and horizontal stress magnitudes are highly anisotropic, and the horizontal to vertical stress ratio (k) varies greatly.

Monitored tunnel deformations

There are two major reasons for a series of instability problems that have occurred in the headrace tunnel at Kaligandaki. First, the rock mass is very weak, schistose, folded, and thinly foliated, with a high degree of strength anisotropy. The second reason is the magnitude of the stress and the degree of stress anisotropy. Due to the low strength of the rock mass against induced stresses, moderate to high deformation in the tunnel wall and crown were recorded despite the application of heavy rock support. The recorded displacement ranged from a few centimeters to nearly a meter. It should be emphasized that the monitored deformation was significantly higher at the spring level of the tunnel walls than in other areas of the tunnel periphery. Figure 4 shows recorded deformations at the spring level of the headrace tunnel chainages. The magnitudes of the tunnel deformations are presented in the form of the total strain for a stretch of the tunnel where the strain exceeded 2 %, representing minor to severe squeezing conditions as defined by Hoek and Marinos (2000). The figure shows total deformation, which was monitored immediately after the rock support was applied until the final concrete lining stage was carried out after several months of tunnel excavation.

Evaluation of tunnel deformations

In an advancing tunnel, the prime focus is on the immediate stability of a tunnel. However, the requirements of the applied rock support will differ according to the stress conditions in situ and the rock mass strength. Stress anisotropy may lead to a situation in which the applied support may experience varying magnitudes of support pressure in the periphery of a tunnel section. In view of this, the effects of stress anisotropy and support requirements were evaluated using both CCM and numerical modeling for the headrace tunnel of the Kaligandaki project.

Estimation of rock mass strength

For any tunnel stability analysis, proper estimation of the input parameters is absolutely crucial. The uniaxial compressive strength (σ_{ci}) of intact rock is one of the most important parameters considered in such an analysis. Laboratory-tested uniaxial compressive strength (UCS) records for some chainages of the Kaligandaki headrace tunnel are available (NEA 2002). Table 2 summarizes the minimum, maximum, and average values of the UCS for two main rock types through which the headrace tunnel passes (Fig. 1). The test results show that the uniaxial compressive strength varies according to the rock type considered as well as among samples of the same rock type. These laboratory-tested strength results are applicable to rocks in squeezed and unsqueezed tunnel sections.

Deformation monitoring was carried out in at least 198 different tunnel sections. The measured tunnel deformations were converted to tunnel strain, which ranged from 0.1 to 9 %. Actual recorded deformations in these 198 tunnel sections were used to back-calculate rock mass strengths using the approach of Hoek and Marinos (2000). Based on these back-calculated rock mass strengths, the uniaxial compressive strengths of intact rocks at corresponding chainages were also back-calculated using equations suggested by Hoek et al. (2002). The back-calculated UCS values were found to be very close to the laboratory-tested results presented in Table 2. In a few

Table 2 Uniaxial compressive strengths of laboratory samples and intact rocks at monitored tunnel chainages

Rock type	UCS of laboratory-tested samples (MPa)[a]				Back-calculated UCS of intact rock at monitored sections (MPa)			
	Minimum	Mean	Maximum	Standard deviation	Minimum	Mean	Maximum	Standard deviation
Graphitic phyllite	8	53	114	28	17	47	101	21
Siliceous phyllite	14	33	80	18	14	57	115	36

[a] Source: NEA (2002)

tunnel sections (chainages 1 + 398, 1 + 806, and 1 + 826 m) where the recorded tunnel deformations were rather low (1.6–2 cm), the back-calculated UCS values exceeded 100 MPa. This may be explained by the fact that the rock mass in these chainages consisted of series of quartz veins within schistose phyllite, which may have led to a low degree of tunnel deformation. In tunnel sections where the tunnel strain was more than 2 %, the minimum, mean, and maximum values of UCS were 14, 36, and 64 MPa, respectively. The back-calculated UCS values at all of these headrace tunnel chainages are also shown in Fig. 4.

In view of the highly schistose and poor-quality rock mass, it was assumed that the rock mass is elastic–perfectly plastic. Following Hoek et al. (2002), it was also assumed that the rock mass obeys Hoek and Brown's failure criterion. The uniaxial compressive strengths of the rock mass (σ_{cm}) were computed using known geological strength indices (GSI) obtained from the tunnel logs prepared during tunnel excavation, a material constant (m_i) of 7, a disturbance factor (D) of 0.5, and a Young's modulus (E_{ci}) ranging from 7.48 to 35.4 GPa with an estimated average of 19.94 GPa, which is close to the average value for graphitic and siliceous phyllite obtained by Panthi (2006). The rock mass deformation modulus (E_{rm}) was computed using the equations suggested by Hoek and Diederichs (2006). Bulk and shear moduli were computed using a Poisson ratio (ν) of 0.1. Following Crowder and Bawden (2004), the dilation angle (ψ) was considered to be one-quarter the friction angle when the GSI value was more than 30; dilation was not considered for the weak rock mass otherwise.

Rock support interaction analyses were performed to estimate the support pressure for three selected overburdens (230, 560, and 620 m) using the mean laboratory-tested UCS values presented in Table 2. Interaction analysis with the average vertical and horizontal stresses showed that the effective support pressure would be 0.5 MPa at an overburden of 230 m and 1.2 MPa at an overburden of 600 m. It is worth underlining here that the effective support pressure for a better-quality rock mass is generally lower than that for a poorer-quality rock mass. This is due to the fact that weaker rock mass tends to deform with high intensity, meaning that extra pressure is directed onto the applied tunnel rock support. This leads us to conclude that the effective support pressures in the applied rock support range between 0.5 and 1.2 MPa, with an average value of 0.8 MPa. The back-calculated values are similar to those documented by Panthi and Nilsen (2007). On the other hand, in tunnel sections with much lower recorded values of tunnel deformation (approximately 17 monitored tunnel sections out of a total of 198), the effective support pressures are estimated to range between 0.1 and 0.4 MPa.

Convergence confinement analysis

Tunnel stability analysis requires an understanding of the behavior of the rock mass against the applied support. CCM is a tool that allows the action of the applied support against deformation in the tunnel contour to be analyzed. The main disadvantage of CCM analysis is that it considers a circular tunnel through a homogeneous rock mass in an isostatic stress state. The strength of the method is that three key components—the ground reaction curve (GRC), the support characteristic curve (SCC), and the longitudinal displacement profile (LDP)—can be generated and analyzed. Out of the 198 sections of the Kaligandaki headrace tunnel monitored for deformation, 77 experienced tunnel strains exceeding 2 % (approximately 17 cm, see Fig. 4). These sections were considered relevant for performing elasto-plastic analyses using the method suggested by Carranza-Torres (2004). The statistical ranges of the input parameters required for this analysis are presented in Table 3.

Deformation in tunnels can be related to the in situ stress, effective support pressure, and shear modulus of the rock mass. Ground reaction curves (GRCs) were prepared for the 77 tunnel sections, assuming the vertical stress (σ_v) to be a uniform (isostatic) stress in situ. The GRC plot (Fig. 5) shows the relationship between the tunnel strain (ε) and the ratio between shear modulus (G) and vertical stress (σ_v) for different possible support pressure (p_i) values. It was found that there must be a power relationship between these parameters that can be fitted fairly well by Eq. 1.

Table 3 Summary of the rock mass parameters used as the input for convergence confinement analysis

Value	Intact rock strength (σ_{ci}) (MPa)	GSI	Rock mass strength (σ_{cm}) (MPa)	Young's modulus (E_{ci}) (GPa)	Modulus of deformation (E_{rm}) (MPa)	Shear modulus (G) (MPa)[a]	Bulk modulus (k) (MPa)[b]
Minimum	13.6	20	0.74	7.5	307	140	128
Mean	36.3	39	2.82	19.9	646	705	646
Maximum	64.4	49	4.28	35.4	2,440	1,109	1,017

[a] $G = \frac{E_{rm}}{2(1+v)}$

[b] $K = \frac{E_{rm}}{3(1-2v)}$

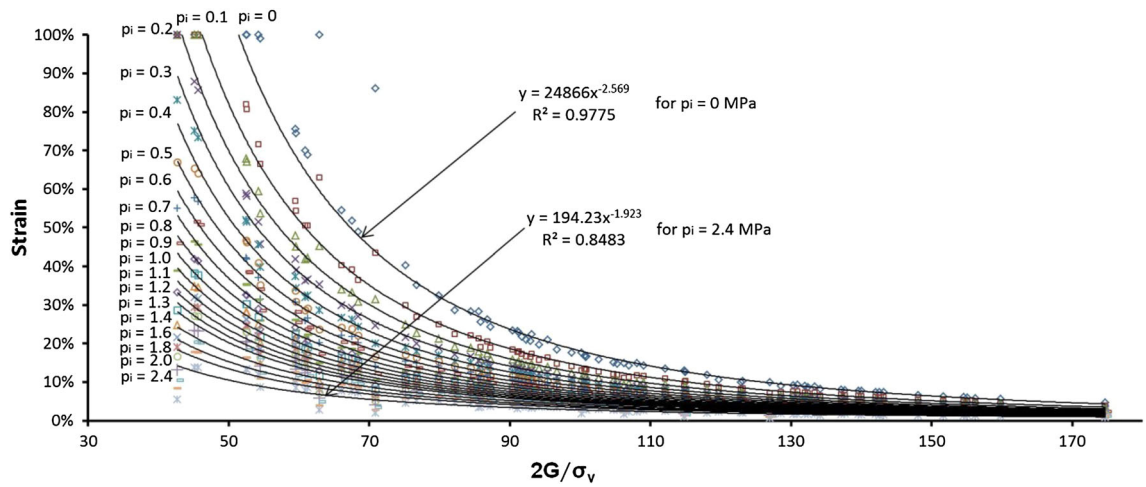

Fig. 5 Estimated tunnel strain curves for corresponding support pressures, based on analytical solutions for isostatic vertical stress

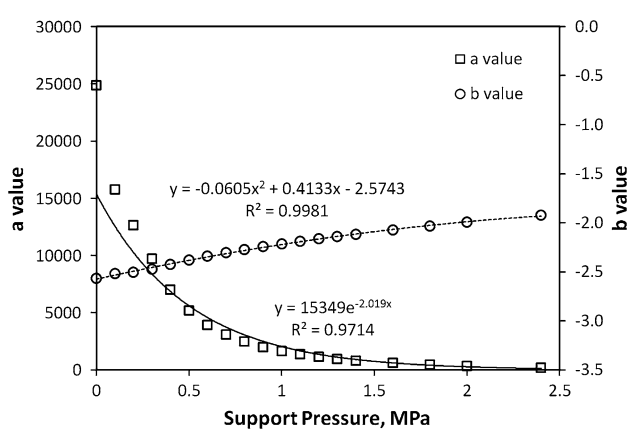

Fig. 6 Variation in trendline constants a and b according to the support pressure, based on analytical solutions for isostatic vertical stress

$$\varepsilon = a\left(2G/_{\sigma_v}\right)^b. \quad (1)$$

In Eq. 1, a and b are constants that vary according to the support pressure, as presented in Fig. 6. These constants can also be estimated for a given support pressure using Eqs. 2 and 3, respectively.

$$a = 15349exp^{-2.019p_i} \quad (2)$$

$$b = -0.0605p_i^2 + 0.4133p_i - 2.5743. \quad (3)$$

The shear modulus (G) of the rock mass can be estimated from the rock mass deformation modulus (E_{rm}) and Poisson's ratio (v). There are many relationships that can be used to estimate the rock mass deformation modulus. However, for a schistose and deformable rock mass such as that around the Kaligandaki headrace tunnel, the relationship suggested by Panthi (2006, 2012) is recommended.

In Fig. 7, back-calculated support pressures obtained using Eqs. 1–3 for recorded tunnel deformations are presented for two different situations: for vertical stress as a uniform stress or an average stress (the average of the vertical and horizontal stresses). It should be noted that the measured tunnel deformations are mostly at the spring level of the tunnel and represent maximum values of the tunnel periphery.

As seen in Fig. 7, the support pressures estimated using the CCM method with the average stress are much lower in magnitude than those computed considering vertical stress as a uniform stress. One of the basic assumptions of the CCM approach is that in situ stresses are always in the isostatic state. However, stress magnitudes around the tunnel periphery are seldom isostatic. Therefore, it is important that both vertical and horizontal stress magnitudes are incorporated into analyses of tunnel deformation

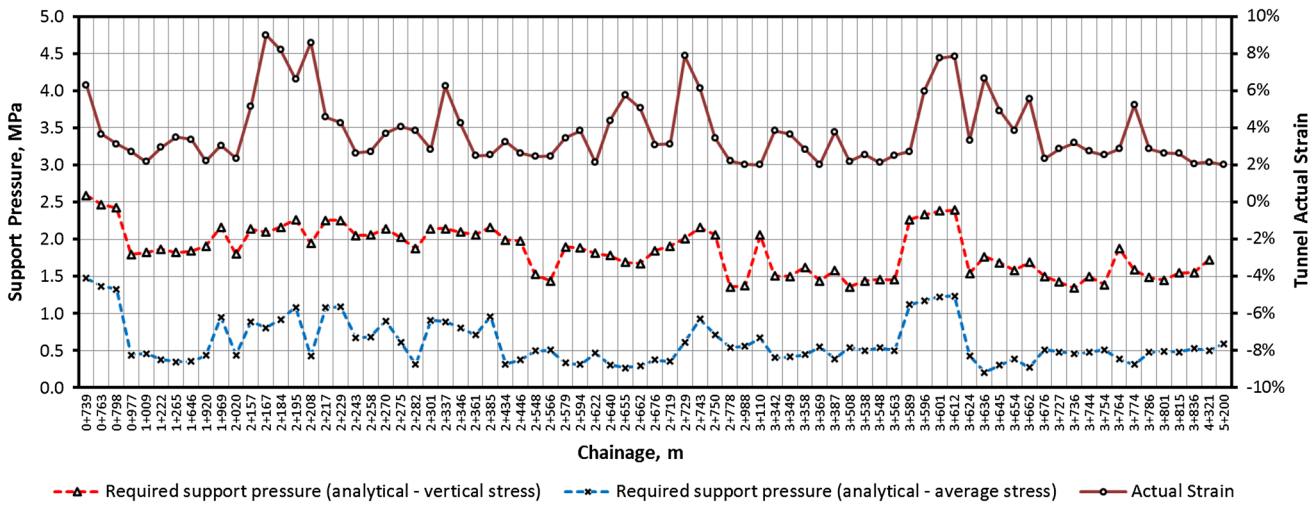

Fig. 7 Required support pressures based on analytical methods

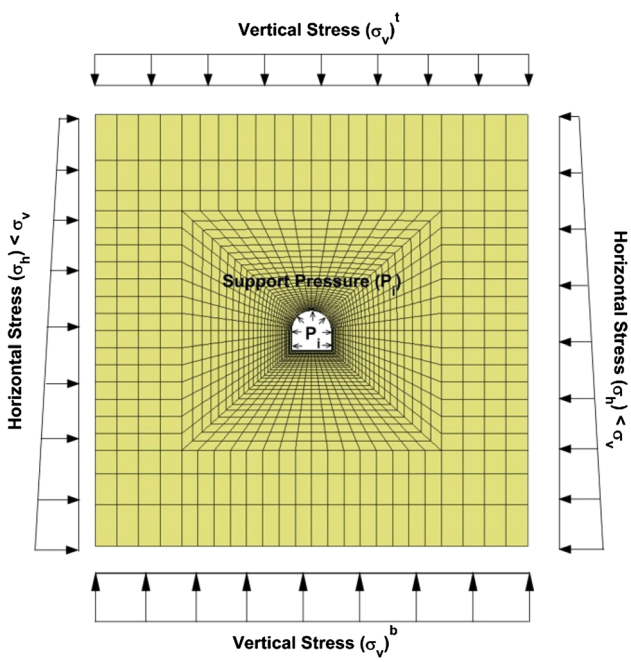

Fig. 8 Numerical model and stress setup

and required support pressures. Numerical analysis is the best tool to assess the effect of stress anisotropy in a noncircular tunnel, such as the Kaligandaki headrace tunnel.

Numerical modeling

3D numerical modeling analysis is time-consuming. Therefore, it was not possible to assess all 177 tunnel sections. Twelve representative inverted-D-shaped tunnel sections were selected for the numerical analysis. A FLAC^{3D} (Itasca 2009) plane strain model was developed (Fig. 8) for each of these tunnel sections. Vertical and horizontal stresses at each section were computed based on the principle discussed in "In situ stress condition." The rock mass was assumed to satisfy the Hoek and Brown failure criterion. The Hoek and Brown parameters m_b, s, and a were computed using equations suggested by Hoek et al. (2002). Table 4 presents input parameters used for the analysis.

As indicated in Table 4, the variation in the magnitude of vertical stress is quite considerable. Horizontal to vertical stress ratios (k) varied from 0.22 to 0.38, pointing to a high degree of stress anisotropy. Similar to the CCM analysis carried out in "Convergence confinement analysis," various support pressures ranging from 0 to 2.4 MPa were applied to generate GRCs. Inverts of the tunnel were left unsupported to match the actual tunneling conditions. Deformations at the crown and the spring level were recorded for each of the tunnel sections for the respective support pressures. The results for the six most representative ground reaction curves (GRCs) among the twelve sections indicated in Table 4 that represent different stress anisotropy (k) scenarios are presented in Fig. 9.

As seen in Fig. 9, CCM analysis with uniformly distributed vertical stress gave the highest deformations in all six tunnel sections. When the degree of stress anisotropy was reduced (i.e., the k value shifted closer to 1), deformation values at the tunnel crown analyzed by numerical modeling were similar to the values calculated by CCM analysis considering isostatic average stress. On the other hand, the deformation values analyzed via numerical modeling at the spring level are lower than the values calculated by the CCM method assuming isostatic vertical stress but higher than those obtained assuming isostatic average stress. This is an interesting observation, as the latter case generally represents the actual situation in most

Table 4 Input parameters for the tunnel sections selected for numerical modeling

Chainage (m)	Vertical stress (σ_v) (MPa)	In-plane horizontal stress (σ_{hi}) (MPa)	In-plane stress ratio (k)	Hoek and Brown parameters			Intact strength (σ_{ci}) (MPa)	Bulk modulus (K) (MPa)	Shear modulus (G) (MPa)
				m_b	s ($\times 10^{-4}$)	a			
0 + 739	6.53	2.49	0.38	0.1551	0.233	0.544	18.7	127.9	139.5
0 + 977	7.15	2.56	0.36	0.5611	8.53	0.507	13.6	376.4	410.6
1 + 222	9.58	2.83	0.30	0.4638	5.00	0.509	21.9	466.3	508.7
2 + 167	16.73	3.62	0.22	0.3323	1.97	0.515	29.1	403.0	439.6
2 + 229	16.75	3.62	0.22	0.2165	0.593	0.527	59.7	525.6	573.4
2 + 275	16.05	3.55	0.22	0.3485	2.25	0.514	41.2	604.7	659.7
2 + 361	15.49	3.48	0.23	0.3168	1.72	0.516	55.7	728.8	795.0
2 + 729	14.43	3.37	0.23	0.3833	2.94	0.512	23.8	394.4	430.3
3 + 612	12.68	3.17	0.25	0.1968	4.54	0.531	32.3	262.4	286.3
3 + 645	12.25	3.12	0.26	0.5101	6.53	0.508	21.1	511.5	558.0
3 + 754	12.87	3.19	0.25	0.5611	8.53	0.507	30.5	844.6	921.4
4 + 321	10.90	2.97	0.27	0.4638	5.00	0.509	31.4	670.1	731.1

squeezed tunnels that pass through a varying rock overburden.

An attempt was also made to check whether there are relationships between the tunnel strain at the spring level (ε_{spl}), the shear modulus (G), the vertical stress (σ_v), and the stress anisotropy coefficient (k). The results of this analysis are presented in Fig. 10. A generalized relationship incorporating stress anisotropy was established (Eq. 4). The vertical stress (σ_v) is multiplied by $(1 + k)/2$ such that the denominator in Eq. 4 represents the effect of horizontal stress. When k reaches 1, the denominator becomes equal to the vertical stress. The coefficients a_{spl} and b_{spl} of this relationship vary according to the effective support pressure (p_i), as indicated in Fig. 11. These constants can be calculated directly using Eqs. 5 and 6.

$$\varepsilon_{spl} = a_{spl}\left(\frac{2G}{\{\sigma_v(1+k)/2\}}\right)^{b_{spl}} \quad (4)$$

$$a_{spl} = 742.23p_i^2 - 1870.6p_i + 1654.7 \quad (5)$$

$$b_{spl} = -0.1541p_i^2 + 0.2022p_i - 2.0003. \quad (6)$$

To verify the validity of these equations, the actual measured tunnel deformation values and rock mass parameters presented earlier were used to back-calculate the effective support pressure at the spring level of the tunnel for all 77 tunnel sections (Fig. 12). The calculated effective support pressures ranged from 0.27 to 2.51 MPa, with an average of 0.84 MPa. The effective support pressures were found to be highest in tunnel sections 0 + 739, 0 + 763, and 0 + 799 m, where the rock mass is faulted. Excluding these three exceptions, the calculated effective support pressure never exceeded 1.63 MPa, which shows that the proposed equations provide good fits within the range of measured effective support pressures documented by Panthi and Nilsen (2007).

Figure 13 shows the tunnel strains computed using Eqs. 1–6 for required support pressures corresponding to actual measured tunnel deformations. The results of this analysis show that the values of tunnel strain computed using Eqs. 1 and 4 with k equivalent to 1 are fairly similar. However, note that the tunnel strain values calculated using these equations are mostly higher than those actually recorded in the tunnel. On the other hand, Fig. 13 clearly shows that the tunnel strain values calculated using Eq. 4 with various k values are very close to the tunnel strains calculated from the actual measured tunnel deformations.

It is evident that the tunnel strain within the periphery of a tunnel depends upon the stress anisotropy and shape of the tunnel. This phenomenon was in fact observed in every monitored section of the Kaligandaki headrace tunnel, where the maximum displacements usually occurred at the spring level of the tunnel. This means that the pressure experienced by the support applied in the tunnel depends upon the magnitude of the stress anisotropy.

Deformation prior to support application

Deformation occurs in an advancing tunnel both ahead of and behind the tunnel face. The deformation of the tunnel will depend on the position of the advancing tunnel face. If the deformation in the tunnel is assumed to be maximum at four times the tunnel diameter behind the tunnel face, the deformation at the tunnel face will be approximately 30 % of the maximum displacement (Carranza-Torres and

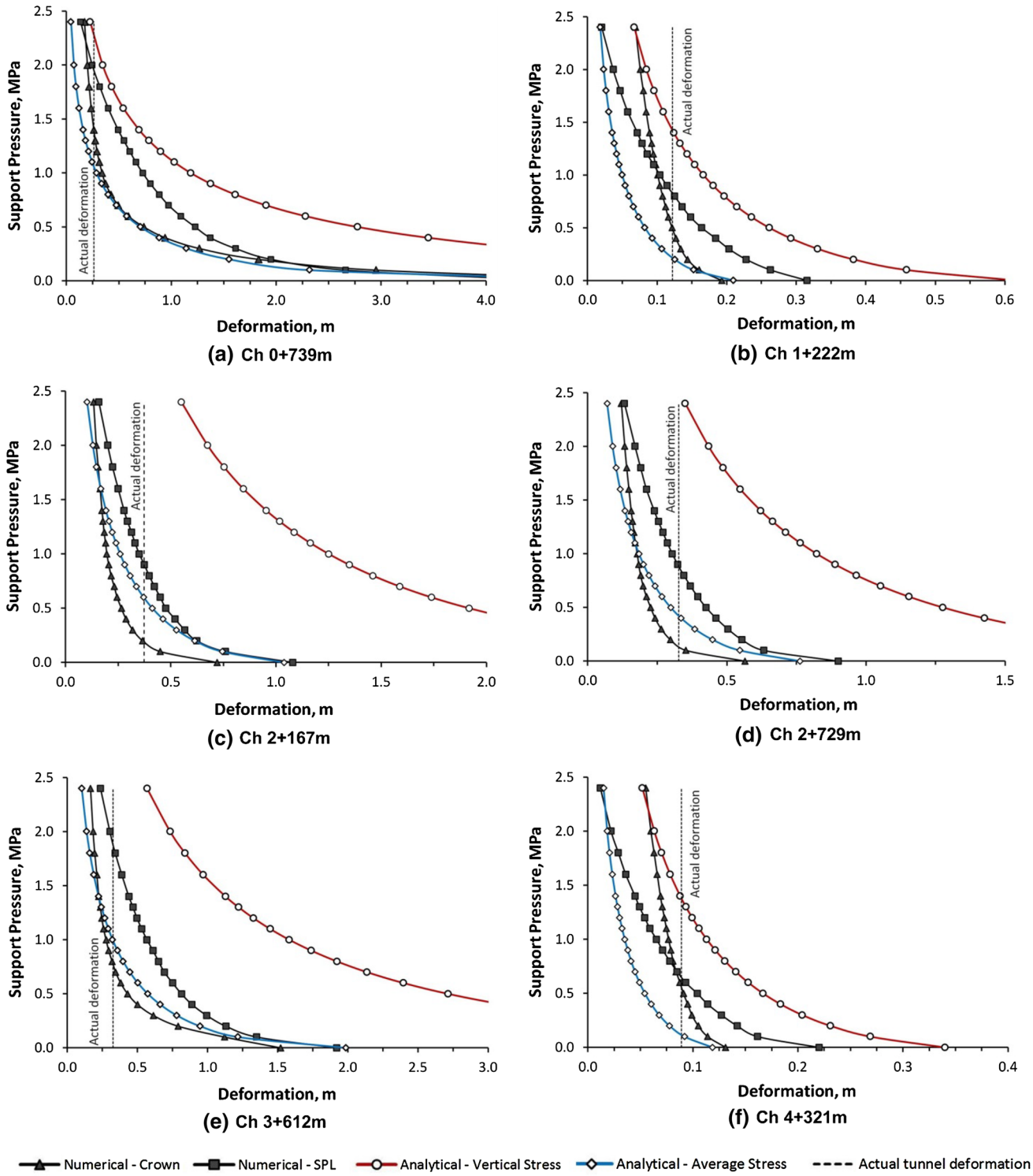

Fig. 9 Comparative ground reaction curves of selected tunnel sections

Fairhurst 2000). Vlachopoulos and Diederichs (2009) suggested an improved longitudinal deformation profile (LDP) for unsupported tunnels that can be used to estimate the deformation in a tunnel when the support is applied. One of the most important assumptions made in this analysis is that stresses around the tunnel are isostatic (uniformly distributed). However, the displacement prior to support application in an inverted-D tunnel in a

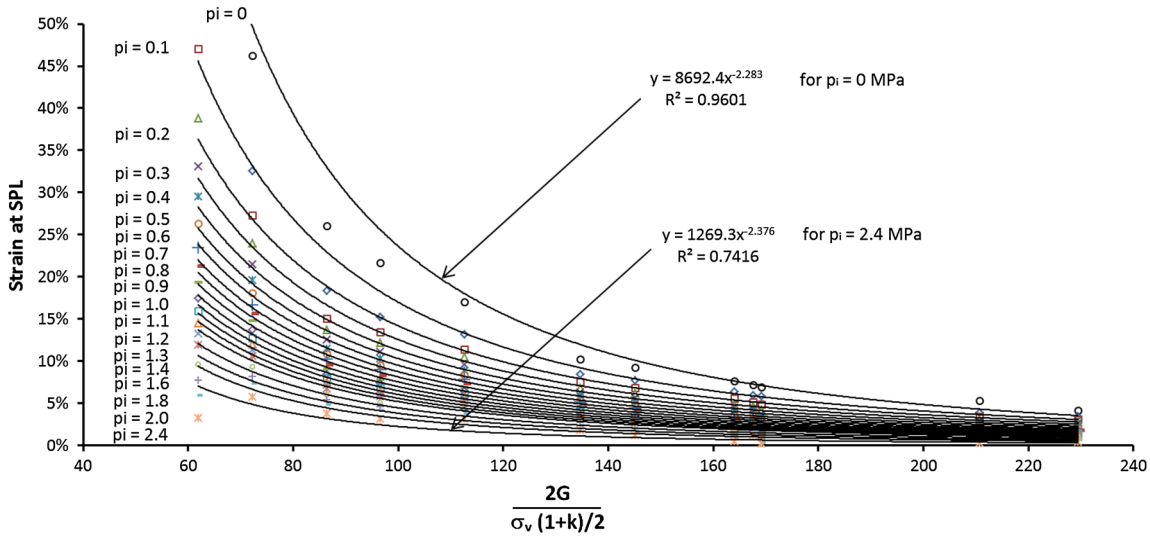

Fig. 10 Estimated tunnel strain curves for particular support pressures at spring level, obtained through numerical solution

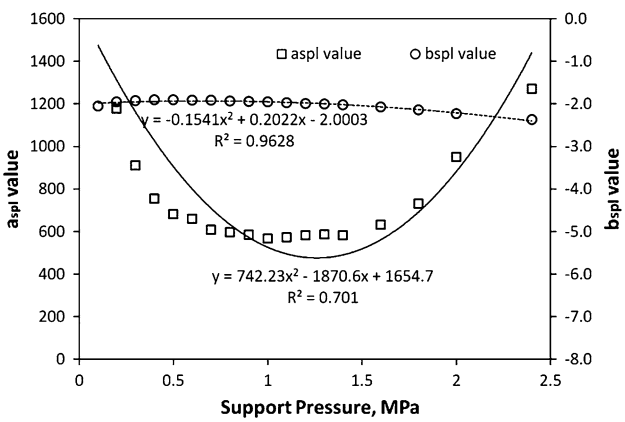

Fig. 11 Variations in the trendline constants *a* and *b* at spring level, obtained through numerical solution

nonuniform stress state will be different from that estimated under isostatic stress conditions. To explore this variation, FLAC^{3D} numerical analysis of headrace tunnel chainage 2 + 167 m (used as an example) was carried out, where the stress ratio k is 0.22. The results of the analysis are presented in Table 5 and Fig. 14. As seen in the figure, the tunnel experiences significantly less displacement during support application than seen in the analysis carried out assuming vertical stress to be uniformly distributed (i.e., in the isostatic stress state).

Figure 14 further indicates that the tunnel experiences a deformation (U_n) prior to support application of approximately 0.18 m at the spring level when the tunnel face is advanced by one meter. This is almost one-third of the displacement (U_a) computed analytically assuming vertical stress in the isostatic state. The actual measured total displacement in this tunnel section was 0.38 m, which corresponds to an effective support pressure of 0.90 MPa as calculated by numerical modeling, or 0.98 MPa when calculated using Eq. 4. On the other hand, the required support pressure would be much higher if the calculation was performed assuming vertical stress to be in the isostatic state.

Conclusion

Understanding the ground's response to support application is important when constructing tunnels through squeezing rocks. It is a well-known fact that there is considerable uncertainty about this response due to the analytical methodology used and the accuracy of the estimated input variables. It is important that the analytical methods used in this context are tested using actual monitored deformation data, mapped geological conditions, and lab-tested rock mechanical properties. An erroneous understanding of the suggested methods may lead to inaccurate interpretation of the deformation magnitude and the effective tunnel support pressure required.

The analysis carried out in this manuscript demonstrates that stress anisotropy exerts a strong influence on the magnitude of tunnel deformation. As demonstrated by this analysis, a traditional CCM analysis that assumes an isostatic stress state generally yields much larger deformations, so the results obtained using it should be considered conservative. The best approach is to conduct a 3D numerical assessment using well-mapped engineering geological information, laboratory-tested mechanical properties of the rock mass, and stress magnitudes that are

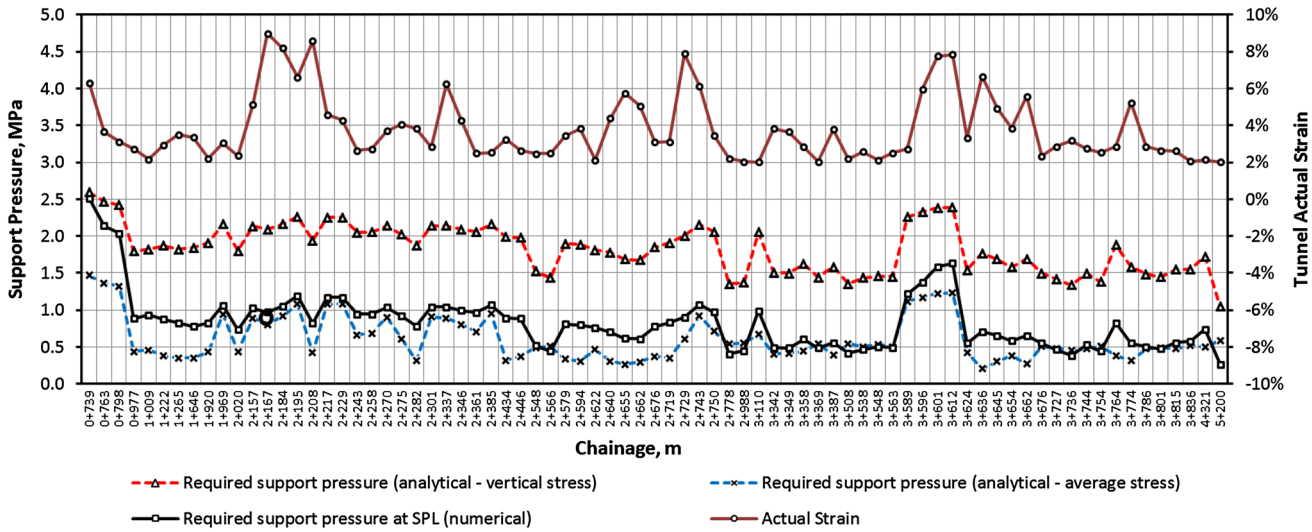

Fig. 12 Required support pressures, as calculated using analytical methods and numerical modeling

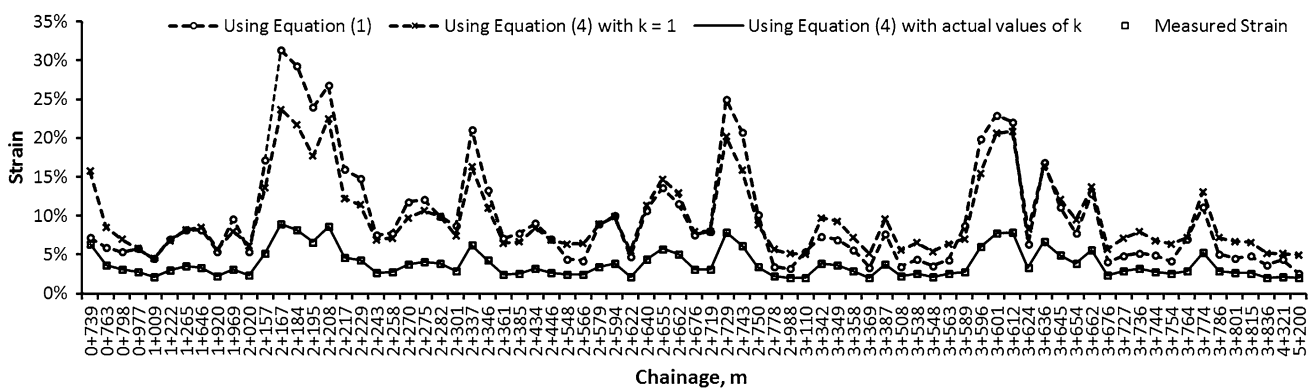

Fig. 13 Comparative tunnel strains under isostatic and anisotropic stress conditions

Table 5 Deformations behind the face at tunnel chainage 2 + 167 m

Location	Deformations at 1 m behind the face (m)		
	Actual stress, unsupported tunnel (FLAC^{3D} numerical result)	Isostatic vertical stress, unsupported tunnel (FLAC^{3D} numerical result)	Isostatic vertical stress calculated using the equations of Vlachopoulos and Diederichs (2009)
Crown	0.20	0.52	0.54
Spring level	0.18	0.51	0.54

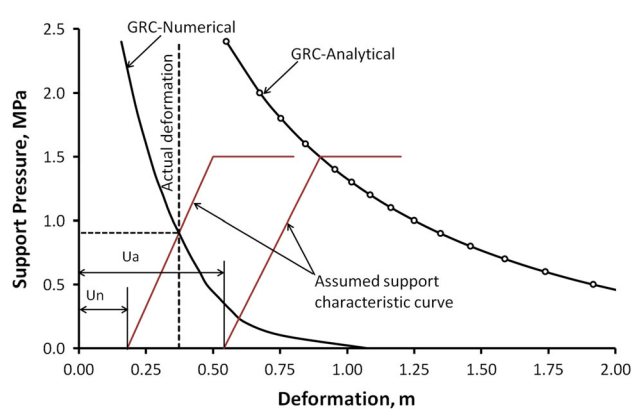

Fig. 14 Rock support interaction at chainage 2 + 167 m

measured or carefully estimated in situ. In addition, Eq. 4 can be used to estimate the magnitudes of tunnel deformations in actual cases with varying stress conditions in situ. However, it should be emphasized here that the proposed equations must be validated using data from many other well-monitored tunnel projects in order to improve the prediction accuracy.

References

Carranza-Torres C (2004) Elasto-plastic solution of tunnel problems using the generalized form of the Hoek–Brown failure criterion. Int J Rock Mech Min Sci 41(3):480–481

Carranza-Torres C, Fairhurst C (2000) Application of the convergence–confinement method of tunnel design to rock masses that satisfy the Hoek–Brown failure criterion. Tunn Undergr Space Technol 15(2):187–213

Crowder JJ, Bawden WF (2004) Review of post-peak parameters and behavior of rock masses: current trends and research. Rocnews, fall. http://www.rockscience.com

Detournay E, John CMS (1988) Design charts for a deep circular tunnel under non-uniform loading. Rock Mech Rock Eng 21:119–137

Goel RK, Jethwa JL, Paithankar AG (1995) Indian experience with Q and RMR systems. Tunn Undergr Space Technol 10:97–109

Hoek E, Diederichs MS (2006) Empirical estimation of rock mass modulus. Int J Rock Mech Min Sci 43:203–215

Hoek E, Marinos P (2000) Predicting tunnel squeezing problems in weak and heterogeneous rock masses. Tunn Tunn Int 32(11):45–51 [32(11): 34–46]

Hoek E, Carranza-Torres C, Corkum B (2002) Hoek–Brown failure criterion—2002 edition. In: Proc N Am Rock Mech Soc Meet, 8–10 July 2002, Toronto, Canada

Itasca (2009) FLAC3D user's manual. http://www.itascacg.com

Nepal KM (1999) A review of in situ testing of rock mechanical parameters in hydropower projects of Nepal. J Nepal Geol Soc 19:1–8

Nepal Electricity Authority (NEA) (2002) Kaligandaki A hydroelectric project—project completion report: vols I-C (headrace tunnel); IV-A (geology and geotechnical); V-C (geological drawings and exhibits). Kathmandu, Nepal

Pan Y, Chen Y (1990) Plastic zones and characteristic-line families for openings in elasto-plastic rock mass. Rock Mech Rock Eng 23:275–292

Panet M (1995) Le calcul des tunnels par la méthode convergence-confinement. Presses de I'ENPC, Paris

Panet M (2001) Recommendations on the convergence confinement method. Association Française des Travaux en Souterrain (AFTES), Paris, pp 1–11

Panthi KK (2006) Analysis of engineering geological uncertainties analysis related to tunnelling in Himalayan rock mass conditions. Doctoral thesis. Department of Geology and Mineral Resources Engineering, Norwegian University of Science and Technology, Trondheim

Panthi KK (2012) Evaluation of rock bursting phenomena in a tunnel in the Himalayas. Bull Eng Geol Environ 71:761–769. doi:10.1007/s10064-012-0444-5

Panthi KK, Nilsen B (2007) Uncertainty analysis of tunnel squeezing for two tunnel cases from Nepal Himalaya. Int J Rock Mech Min Sci 44:67–76

Singh B, Jethwa JL, Dube AK, Singh B (1992) Correlation between observed support pressure and rock mass quality. Tunn Undergr Space Technol 7(1):59–74

Vlachopoulos N, Diederichs MS (2009) Improved longitudinal displacement profiles for convergence confinement analysis of deep tunnels. Rock Mech Rock Eng 42:131–146